
Improving Local Training in Federated Learning via Temperature Scaling

Kichang Lee, Songkuk Kim, JeongGil Ko

School of Intergrated Technology, Yonsei University

{kichang.lee, songkuk.kim, jeonggil.ko}@yonsei.ac.kr

Abstract

Federated learning is inherently hampered by data heterogeneity: non-i.i.d. training data over local clients. We propose a novel model training approach for federated learning, *FLex&Chill*, which exploits the *Logit Chilling* method. Through extensive evaluations, we demonstrate that, in the presence of non-i.i.d. data characteristics inherent in federated learning systems, this approach can expedite model convergence and improve inference accuracy. Quantitatively, from our experiments, we observe up to $6\times$ improvement in the global federated learning model convergence time, and up to 3.37% improvement in inference accuracy.

1 Introduction

Federated learning represents a paradigm enabling the training of effective models within distributed environments without explicitly exposing local data McMahan et al. [2017]. This approach provides opportunities for communication and computation efficiency during training by sharing model parameters/gradients learned independently from local learning processes while suppressing raw data transmissions. Furthermore, since training operations take place in a decentralized manner, federated learning opens the possibility of parallelizing the model training process via the assistance of local client devices. It presents an attractive solution for handling and exploiting the vast amounts of data generated by many mobile and Internet of Things (IoT) device entities consisting of the overall system Park et al. [2023a].

In contrast to conventional centralized training methods, federated learning faces challenges associated with delayed model convergence and limited performance. A fundamental challenge of federated learning arises from the disparity of training data used at each client device. Federated stochastic optimization encounters difficulties in determining optimal parameters, leading to increased communication overhead between local devices and the central server, as well as the need for additional training on (typically resource-limited) local devices Zhao et al. [2018].

To address these challenges, a number of prior research have focused on optimizing local training operations on federated learning clients or on refining the server-side aggregation process. For instance, FedProx Li et al. [2020] controls the number of local device iterations, aiming to train models resilient to challenges posed by non-independent and non-i.i.d. data environments. SCAFFOLD Karimireddy et al. [2020] achieves expedited convergence and improved model accuracy McMahan et al. [2017] by introducing a correction term in the model aggregation phase to balance the influence of each client. These operations alleviate challenges posed by the non-i.i.d. environment, a common dataset configuration for federated learning clients.

This paper proposes a novel model training approach for federated learning, *FLex&Chill* (Federated Learning **EX**ploiting logit **CH**illing), that targets to boost the convergence and model performance via temperature scaling, namely *logit chilling*, during the local model training operations. Note that a typical neural network generates a probability (p_i) for each class from its neural network logits (z_i) by applying a softmax operation (Eq. 1) with the temperature T conventionally set to 1. However,

it is not uncommon in other application scenarios to exploit even higher temperature values (i.e., $T \in (1, \infty)$), for example, in knowledge distillation Hinton et al. [2015], Touvron et al. [2021] or neural network calibration Guo et al. [2017].

$$\xi(z, i, T) = p_i = \frac{\exp(z_i/T)}{\sum_j \exp(z_j/T)} \quad (1)$$

When employing a temperature $T > 1$, the probability distribution across classes undergoes smoothing due to the narrowed interval between logits Guo et al. [2017], making such an approach suitable for applications such as knowledge distillation. Notably, despite altering the probabilities, the order of labels’ probability remains unaffected with respect to changes in T . While these works successfully explore the impact of varying temperatures for neural network operations, they mainly focus on applying high temperatures *after* the model training process, mostly for inference operations. Since increasing T reduces the training confidence, such schemes are effective in taming overconfident DNNs.

On the other hand, in federated learning, where disparate training data is common, *increasing model confidence* of each individually trained client model (using small T) prior to parameter aggregation can be a more effective approach. Our investigation involves measuring both the gradient flow and data position shift within the representation space to provide guidelines in this unexplored territory.

Specifically, this work targets to show that utilizing fractional temperature values (i.e., $T \in (0, 1)$) during the training process enables effective gradient propagation towards the input layer when applied to federated learning data distribution scenarios. Consequently, we observed that lower temperatures facilitate more efficient data updates within the representation space when dealing with non-i.i.d. datasets, a common characteristic of federated learning systems. From our evaluations with three datasets and three baseline federated learning models, we show that these effects accelerate the federated learning model convergence time by up to **6.00** \times and improve the inference accuracy by up to **3.37**%, despite potential concerns on model instability when training with with low temperatures. We summarize the contributions of this work in three-fold as the following:

- To the best of our knowledge, this is the first work that explores the impact of integrating temperature scaling during the training process in a federated learning scenario.
- We offer empirical evidence that demonstrates the performance enhancements of exploiting *logit chilling* in federated learning scenarios, by examining the gradient flow and data position shifts within the representation space.
- We introduce a novel federated learning model training approach, *FLex&Chill*, showcasing the application of low temperature usage during the training process.

2 Background and Related Work

2.1 Temperature scaling

In machine learning, a model’s output probability distribution serves diverse purposes. Primarily, classification models offer probabilities for each class, showcasing the model’s confidence in its predictions. This certainty measure allows consideration of the likelihood of each class prior to making a final classification decision. Moreover, this distribution offered by the model helps in understanding the uncertainty of a model on its decisions Park et al. [2023b], Pearce et al. [2021].

For neural networks, computing probabilities from logits often involves employing softmax operations, as in Eq. 1. Here, the temperature parameter ($T > 0$) controls the probability distribution’s concentration towards one class, and manages how the categorical probability is dispersed over possible classes Jang et al. [2016]. Notably, this categorical probability aligns with the concept of entropy in information theory, offering a perspective where T governs the level of disorder or uncertainty within the distribution. Specifically, with $T \in (1, \infty)$, the probability distribution tends to be smoother as T increases. This arises from the diminished differences between logit values, enhancing the distribution’s entropy. In contrast, $T \in (0, 1)$ sharpens the probability distribution, since a lower T amplifies inter-logit differences, effectively polarizing the distribution and concentrating probabilities closer to the maximum logit value. Consequently, model predictions are made more confidently, by allocating higher probabilities to fewer classes, thereby reducing uncertainty in the distribution.

Therefore, temperature scaling operates as a means to adjust the probability distribution within a neural network-based system. Previous work in Knowledge Distillation Hinton et al. [2015], Touvron et al. [2021] exploit the temperature value by applying a high temperature $T \in (1, \infty)$ to

achieve a smoothed probability distribution. This manipulation aims to magnify small values within the distribution, often representing hidden information encapsulated within the model. Additionally, in generative models Shih et al. [2023], Wang et al. [2020], temperature scaling regulates the randomness inherent in model outputs. This technique allows for the control of variability levels in generated samples, enabling adjustments to generated output diversity. Temperature scaling is also used in model calibration Guo et al. [2017]. Applying temperature adjustments to the model’s output probabilities, typically through a scaling factor T , aids in aligning these probabilities more accurately with the true likelihoods or uncertainties present in the data. Likewise, previous work has focused on applying high-temperature values for various purposes, mostly for the purpose of conservatively better understanding the full dataset without bias.

2.2 Federated learning

In recent years, federated learning has emerged as a promising paradigm in machine learning, particularly in scenarios where data privacy, security, and the decentralization of model training are core concerns. Unlike traditional centralized training approaches, federated learning enables model training across distributed devices or servers while keeping the data localized; thus, addressing privacy challenges associated with centralized data aggregation. This decentralized learning paradigm involves iterative model training where local updates occur on individual devices, and only aggregated model updates are shared with the central server.

Despite its benefits, federated learning poses several challenges. A body of work has tackled the issue of communication overhead stemming from the exchange of frequent model parameter updates. A number of previously proposed works have proposed schemes to effectively abstract the model parameters in various forms to relieve the communication and networking overhead Park et al. [2023a]. Furthermore, federated learning systems are prone to facing issues arising from data heterogeneity caused by the diversity or differences in the characteristics, distributions, or formats of data across federated learning clients. Previous works have attempted to address this challenge by addressing relevant issues such as variations in feature/input variations Yu et al. [2021] and spatio-temporal variations Liu et al. [2020].

3 Design of FLex&Chill

We initiate our discussions by exploring the impact of logit scaling, also known as temperature scaling, providing empirical evidence on the rationale behind our proposed system. Furthermore, in this section, we introduce our system, referred to as *FLex&Chill*, a novel local training approach designed for efficiently training a federated learning framework.

3.1 Impact of Training with Lower Temperatures

As aforementioned, conventionally, temperature scaling has primarily been focused on calibrating the probability distribution of a model’s output *after* the model training phase, with a limited exploration into its application *during* the training process itself. In this section, we present empirical results on three initial experiments specifically crafted to showcase the implications of employing temperature scaling throughout the training phase operations in different dimensions. Through these investigations, our aim is to establish a foundation for comprehending the potential implications and advantages associated with the utilization of temperature scaling techniques in neural network training. We conduct our experiments with the CIFAR10 dataset Krizhevsky et al. [2009] and use a 2-layered CNN architecture McMahan et al. [2017] as the baseline neural network architecture. For experimental details, see APPENDIX B

3.1.1 Gradient flow patterns

Our first experiment focuses on assessing the norm of computed gradients within the input layer for various temperature values (T), and we present a sample distribution plot of how the gradients flow for 50K training samples in Figure 1. Note that here we separate the plots for the correctly inferred samples (in the forward pass) and the incorrect ones to observe their differences. The propagation of gradients to the input layer serves as an indicative metric for the model’s learning efficacy. Successful gradient propagation to the input layer implies that the model effectively utilizes and comprehends information from diverse features within the input data during the training phase Evci et al. [2022].

As shown in Figure 1, the mode of distribution shifts to larger values with decreasing temperatures for both correct and incorrect predictions. One reason behind this mode shift stems from the gradient function characteristics of softmax. Eq. 2 presents the gradient of cross-entropy for the softmax

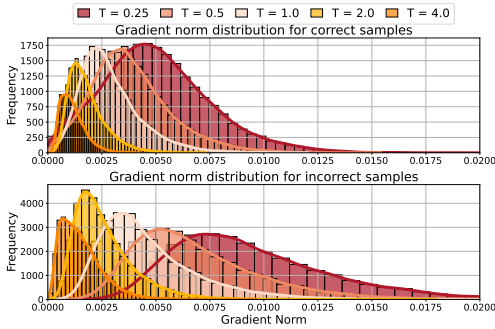


Figure 1: Distribution of gradient norm at input layer for correctly/incorrectly inferred samples with varying training temperatures.

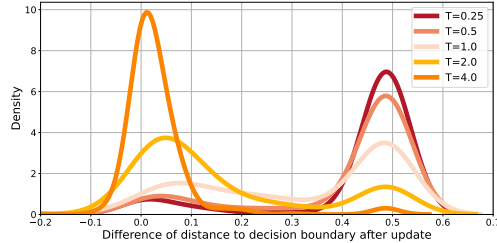


Figure 2: Distributions depicting differences between distances to the decision boundary before and after model updates for varying training temperatures. Notice that lower temperatures show a noticeable shift in estimations’ positions on the representation space, suggesting their aggressiveness in modifying the model even with a small number of training samples.

activation (\mathcal{L}) with varying temperature T and hard target, one-hot encoded labels. For brevity, we present the final derivation result and leave details in the Appendix (see Appendix A). Since the gradient is multiplied by $\frac{1}{T} > 1$, for low temperatures $T < 1$, we can expect a gradient boost.

$$\frac{\partial \mathcal{L}}{\partial z_i} = \frac{1}{T}(p_i - y_i) = \frac{1}{T} \left(\frac{e^{z_i/T}}{\sum_j e^{z_j/T}} - y_i \right) \quad (2)$$

Furthermore, from the perspective of the loss term ($p_i - y_i$), when the model yields an incorrect decision, the loss term significantly increases as $p_i \rightarrow 0$. The double-folded effect accounts for a substantial mode shift with thick and long tails in the gradient distribution for lower temperatures.

3.1.2 Data position shift in the representation space

To better understand the impact of temperature scaling on the training process, we conducted a study into the shift of a data’s position in the representation space (i.e., the distance to the decision boundary). Drawing inspiration from the concept of ‘travel to decision boundary’ as proposed by Kim et al. Kim et al. [2022], we quantified the distance of a data point’s inference result to the decision boundary by determining the magnitude of epsilon (ϵ) value multiplied by the adversarial perturbation Goodfellow et al. [2014] needed to alter the model’s decision.

For this experiment, we configure an initial neural network and perform inference for 1,000 samples to identify the results’ positions on the representation space. Among the 1,000, we select the ones that were misclassified, recompute their positions after performing one training operation using that specific data point, and compute the difference in positions on the representation space concerning the decision boundary. By doing so, we can observe how drastically one training operation affects the next inference output to different temperatures used in the training phase.

Figure 2 plots our results in the form of distributions depicting differences between distances to the decision boundary before and after model updates. When higher temperatures ($T = 2, 4$) are applied, we can notice that the changes in inference results’ positions are not significant (i.e., plots skewed towards 0). Whereas, with a small T , we can notice more pronounced shifts in data positions within the representation space. This suggests that using a small T at the softmax operations can actively steer the model towards (potentially) substantial optimization to better align with the training data.

3.1.3 Visualization in the representation space

To examine the effect of applying a low temperature during the model training phase, we conducted a simple example that classifies 2-dimensional data via logistic regression. We split the data into three different subsets and assign them as three devices with non-i.i.d data. The Softmax layer was applied at different temperatures ($T=1.0, 0.5$) during the local training phase and average model weights for aggregation after 10 local updates.

Figure 3 illustrates the classification boundaries and samples distributed in the representation space for the three clients and the aggregated model. The results suggest that applying $T = 0.5$ effectively reflects the local dataset characteristics compared to $T = 1.0$. Specifically, as an example, for clients 0, 1 and the aggregate model, using $T = 1.0$ fails to make a clear distinction between the red and light green samples; whereas, when applying $T = 0.5$, this distinction becomes pronounced.

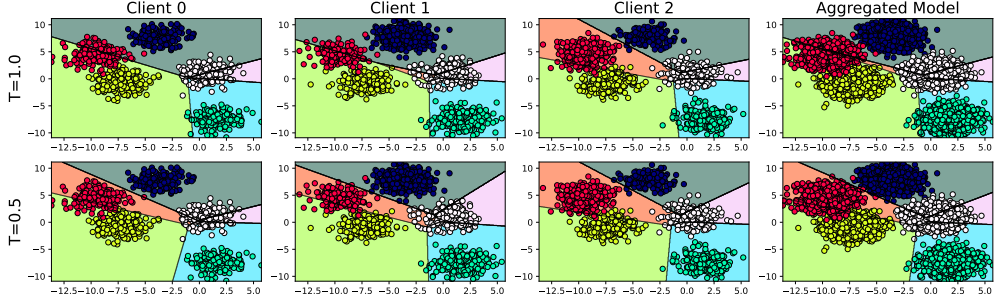


Figure 3: Example of data points in the 2D representation space with their respective classification boundaries for different federated learning clients with varying training temperatures.

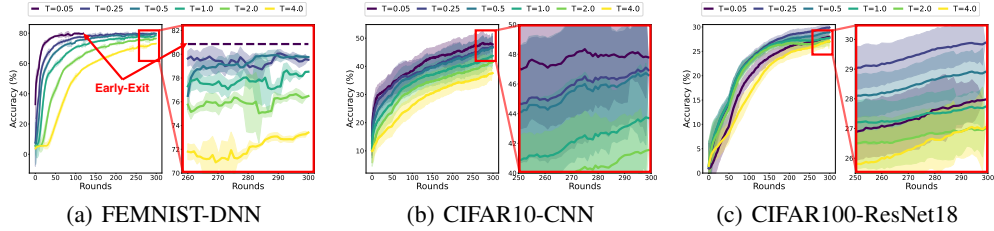


Figure 4: Average federated learning client-side model accuracy for different temperatures used in training. Overall, lower temperatures show higher average model accuracy for federated learning systems.

3.2 *FLex&Chill* and Logit Chilling

Based on such empirical observations, we hypothesize that training neural networks with lower temperatures can benefit the model convergence and performance for systems exploiting non-i.i.d. data, which is common for federated learning scenarios. In *FLex&Chill* we term this as *logit chilling*, as we ‘chill down’ the temperature at the softmax operations, thereby altering the logit computation derived from the neural network during the training process. The focus of a *FLex&Chill*-based federated learning system is to exploit logit chilling to train a client-side model with low-temperature values. As we observed through the studies above and as our evaluations will show, this has an effect of effectively exploiting crucial information from the training samples to actively alter the model towards the new knowledge.

The lower temperatures used by Logit Chilling directly influence the local training process of each federated learning client. Notably, the seamless integration of Logit Chilling and *FLex&Chill* with existing federated learning frameworks is a distinct advantage, allowing for a straightforward implementation within already deployed frameworks. Furthermore, we note that *FLex&Chill* can be used orthogonally with other efforts that accelerate federated learning training operations such as FedProx and SCAFFOLD. For a detailed explanation and experimental result about the orthogonality of *FLex&Chill*, please refer to Appendix C.

4 Experiment

We evaluate the performance of *FLex&Chill* using three datasets: (i) FEMNIST from the LEAF database Caldas et al. [2018a], including the Extended MNIST handwriting data Cohen et al. [2017], (ii) the CIFAR10 dataset, and (iii) the CIFAR100 dataset Krizhevsky et al. [2009]. As metrics, we use the average accuracy and training loss observed at the clients, selected to observe both the performance gain and the effectiveness of *FLex&Chill* in its training operations. Furthermore, we also present the number of federated learning rounds needed to achieve a pre-defined target accuracy.

4.1 Experiment Setup

Dataset. We detail the datasets used in our work as follows.

- **FEMNIST dataset:** The FEMNIST dataset comprises of 10 handwritten digits (0-9) and 52 characters (26 lowercase and 26 uppercase) images contributed by 712 users, totaling 157,132 samples. We selected a subset of 36 users, each with diverse amounts of local data to account for the non-i.i.d. environment. We followed the implementations provided by the original work Caldas et al. [2018b].
- **CIFAR10 and CIFAR100 dataset:** We use baseline CIFAR10 and CIFAR100 datasets Krizhevsky et al. [2009] and manually partition data over 50 federated learning users, with each holding 1,000 samples.

Temperature (T)	FEMNIST-DNN			CIFAR10-CNN			CIFAR100-ResNet18		
	Accuracy (%)	Loss	Num. of Round	Accuracy (%)	Loss	Num. of Round	Accuracy (%)	Loss	Num. of Round
$T = 4.0$	73.60 (-5.06)	0.893	299 (0.44x)	37.58 (-3.76)	1.724	299 (0.84x)	28.05 (-0.20)	2.984	288 (0.69x)
$T = 2.0$	77.20 (-1.46)	0.749	205 (0.64x)	40.35 (-0.99)	1.638	270 (0.93x)	27.89 (-0.36)	2.918	288 (0.69x)
$T = 1.0$	78.66 (0.00)	0.684	132 (1.00x)	41.34 (0.00)	1.594	251 (1.00x)	28.25 (0.00)	2.918	200 (1x)
$T = 0.5$	79.78 (+1.13)	0.654	88 (1.50x)	41.52 (+0.18)	1.551	161 (1.56x)	29.77 (+1.52)	2.875	178 (1.12x)
$T = 0.25$	79.50 (+0.85)	0.650	57 (2.32x)	43.41 (+2.07)	1.532	132 (1.90x)	30.63 (+2.38)	2.997	152 (1.32x)
$T = 0.05$	80.86 (+2.20)	0.643	22 (6.00x)	44.71 (+3.37)	1.528	106 (2.37x)	27.05 (-2.72)	4.228	239 (0.74x)

Table 1: Average classification accuracy, model training loss, and number of federated learning training rounds needed to achieve the maximum accuracy of the $T=4$ cases for each dataset-model combination.

Model. For each dataset, we utilized distinct model architectures, taking into account the specific challenges and characteristics inherent to each dataset. For FEMNIST, an MLP model featuring four linear layers was employed. We term this combination as “FEMNIST-DNN” in the rest of our evaluations. In the case of the CIFAR10 and CIFAR100 datasets, experiments were conducted using a two-layer CNN model McMahan et al. [2017] and a ResNet18 He et al. [2016], respectively. These two cases are denoted as “CIFAR10-CNN” and “CIFAR100-ResNet18.”

Experiment Details. Each case underwent local training for 300 federated training rounds, utilizing FedAvg McMahan et al. [2017] as the baseline federated learning framework. FedAvg is a widely used framework for federated learning. In each round, the server selects 10 participating clients, employing Stochastic Gradient Descent (SGD) as the optimizer with a learning rate of 0.001 Ruder [2016]. Each client trained its model for 10 local epochs, employing a batch size of 16, and utilized cross-entropy loss as the loss function. Unless specified otherwise, the experiment was conducted using the same hyperparameters as mentioned in this section.

4.2 Average Client-side Accuracy

We report the average client-side model accuracy obtained for models trained with different temperatures in Figure 4. For all three datasets (and the three respective models used for each test case) we see an increasing accuracy trend observed for lower temperatures. Note that for the FEMNIST-DNN case with $T=0.05$, we noticed that the accuracy converges after 120 rounds; thus, perform an early exit for this case. One interesting aspect we can notice is that the accuracy for the $T=0.05$ case, which is the lowest temperature we tested for, does not show the best performance for the CIFAR100-ResNet18 experiment. While the $T=0.05$ case shows the best performance of FEMNIST-DNN and CIFAR10-CNN, for CIFAR100-ResNet18, we see an accuracy worse than the $T=0.5$ case. This suggests that training with the lowest possible temperature value is not always ideal, rather this result highlights the importance of identifying a proper training temperature as we will further discuss in Section 5. A closer zoom into the plots suggests that the best-performing configuration can change over the training round and can vary for different datasets, but overall, we can notice that exploiting a temperature value lower than “1” in the training process can help improve the classification accuracy.

The average accuracy for all federated learning clients after 300 training rounds presented in Table 1 confirm our observations, indicating that with $T=0.05$, the CIFAR10 case shows a 3.37% improvement in accuracy compared to the $T=1$ case. Even for other cases, the use of a low-temperature value shows promising results in terms of accuracy. We emphasize once more that this does not mean that the accuracy will always perform better at the lowest temperature. Rather, our results suggest the need to carefully explore the fractional temperature space in the federated learning training process. We note that the performance for model performance and convergence speed tends to be similar regardless of federated learning hyperparameters (see Appendix D).

4.3 Federated Learning Convergence Analysis

Finally, in the last columns for each test case in Table 1 we present the number of federated learning training rounds needed to achieve a preset target accuracy for different temperature values used for model training. This number provides an understanding of how efficient the local training processes are when different temperature values are applied. Specifically, in this experiment, we configure the target accuracy to be the maximum accuracy achieved within 300 training rounds with $T=4$. For example, for the FEMNIST-DNN and CIFAR10-CNN cases, the maximum accuracy for $T=4$ was achieved at the 299th round, while CIFAR100-ResNet18 achieved such accuracy after 288 rounds.

From the results in Table 1 we can notice that with $T=0.05$, the FEMNIST-DNN case achieves the target accuracy after only 22 training rounds. We see similar trends of low temperatures positively affecting the training efficiency throughout our results. This is from the general aggressiveness of training behaviors when applying lower temperature training. Given a single training sample, while

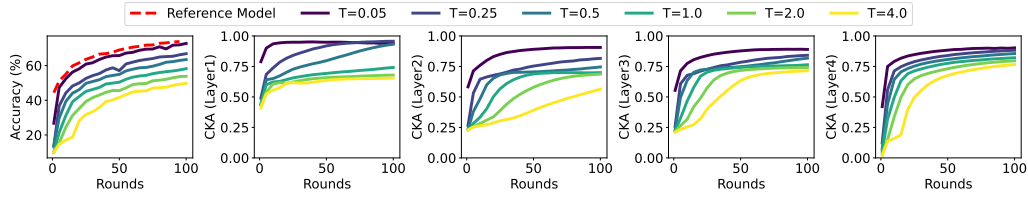
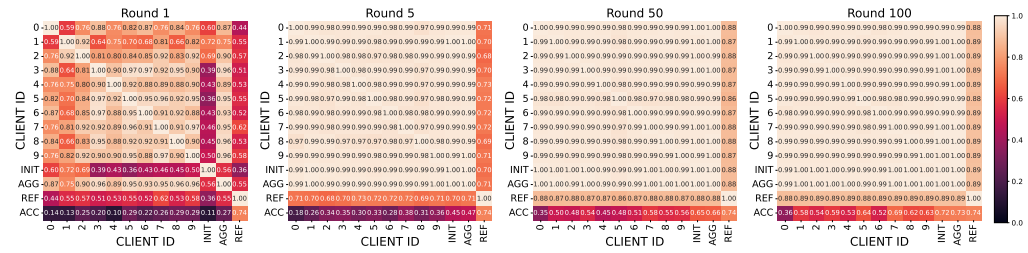
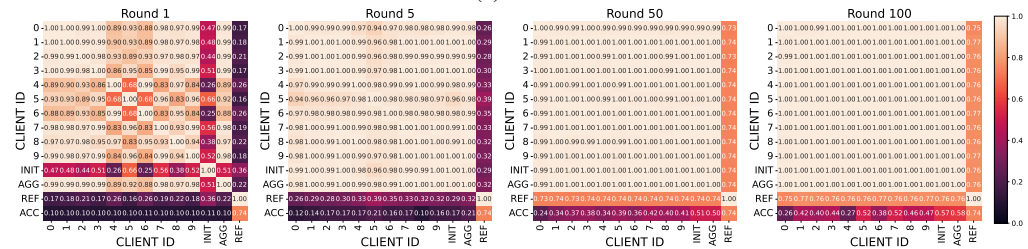


Figure 5: Test accuracy of the global model and feature space similarity in each layer reference model trained with i.i.d. dataset and the global model trained with non-i.i.d. dataset with different temperatures applied during the local training.



(a) $T=0.05$



(b) $T=1.0$

Figure 6: Client-wise feature space similarity matrix measured in penultimate layers by using CKA and inference accuracy in different temperatures (0.05, 1.0) and federated rounds (1, 5, 50, 100). (INIT: Initial dispatched model in the given round, AGG: Aggregated global model, REF: Reference model, ACC: Accuracy)

high temperature-based training conservatively absorbs the available information, lower temperatures are more progressive in making model changes. Given the small datasets used for local training and the need to effectively deliver its knowledge to the server for aggregation, we see *FLex&Chill* as an effective way to train client-side models in the federated learning process.

4.4 Feature Space Similarity Analysis

To better understand the mechanism and rationale behind the performance of *FLex&Chill*, we analyze the similarity of the feature space between global (aggregated) models trained with different temperatures against a reference model trained in an *i.i.d.* data configuration. Specifically, we employ the Centered Kernel Alignment (CKA) Kornblith et al. [2019] for computing the similarity of feature spaces, a widely used approach in evaluating model divergence in federated learning Collins et al. [2022], Luo et al. [2021]. Note that a limitation of CKA measures is that they only report network similarity without considering training quality. Thus, we use a well-trained reference model from an *i.i.d.* environment to observe CKA variations of the penultimate and classification layers between the global models and the reference model.

We note that the reference model is trained with $T=1$, while comparison models (e.g., global models from federated learning) are trained in non-*i.i.d.* environments with different T . In the experiments, we used a 2-layered CNN and the CIFAR-10 dataset as in Section 4.1, with the dataset distributed among 10 clients using a Dirichlet distribution Hsu et al. [2019]. All clients participated in the federated training process. For detailed discussions on the experimental setup and CKA, please refer to Appendix E.

As the accuracy and CKA plots for different layers in Figure 5 show, introducing the non-*i.i.d.* environment itself drops the model accuracy (73.86% \rightarrow 58.19%) at $T=1$, with the CKA of the penultimate/classification layers between the two models remaining at 0.7644/0.8214 after 300 rounds. Nevertheless, with $T=0.05$, despite the dataset disparity, the global model achieved a comparable

accuracy of 72.76% with relatively higher CKA values (0.8898/0.9026) in both the penultimate and classification layers. We point out that improved gradient flows via applying low temperatures help models to learn similar local features (i.e., layers 1, 2), affecting the following layers (i.e., layers 3, 4) in the early stage of the learning process. As a result, applying low temperatures during local training effectively improves the overall accuracy performance in a non-i.i.d. data distribution setting and helps models learn similar feature spaces compared to the ideal i.i.d. data configuration.

We now target to better understand how local model updates progress with different T . For brevity of the paper we only report the CKA at the penultimate layer, and plot all other cases in Appendix E. Specifically, Figure 6 plots the model accuracy (ACC) and measured CKA at the penultimate layer of a client’s local model with (i) the initially distributed model (INIT), (ii) the aggregated model (AGG), (iii) the ideal reference model trained with i.i.d data distribution (REF), and (iv) other client models while $T=0.05$ and 1.0. In Round 1, clients’ local models trained with $T=1$ show high feature space similarity against each other while failing to learn the features of the ideal reference model. With $T=0.05$, the CKA between local models are relatively low while showing high similarity with the reference model. After five rounds (and beyond), local models trained with both $T=1.0$ and $T=0.05$ showed high similarity amongst themselves and the initial/aggregated models, but the $T=0.05$ case continuously shows higher similarity with REF and reports higher accuracy. Hence, we argue that adapting low temperatures allows local models to learn effective and diverse features to quickly converge the federated learning process.

4.5 Impact of Dataset Dispersion and Federated Learning on *FLex&Chill*

We now examine the impact of *FLex&Chill* on different model training configurations. Specifically, using the CIFAR10-CNN test case, we examine two additional configurations: (i) centralized learning with i.i.d. data and (ii) federated learning with i.i.d. data. Note that the federated learning network is identical to our previous experiments except for the dataset distribution and was tested for 300 rounds. By comparing these results with the non-i.i.d. federated learning results, we target to understand the impact of *FLex&Chill* on federated learning and dataset disparity in greater detail.

As Table 2 shows, applying *FLex&Chill*, thus a lower T does not induce a positive impact on the performance of centralized learning scenarios. In fact, for centralized learning, controlling T for the training process does not show a noticeable impact. We see the same phenomena for the federated learning system with i.i.d. samples as well, suggesting that the performance enhancements we see in Table 1 are not an effect of the federated learning process itself.

T	Centralized - i.i.d.		Federated - i.i.d.		Federated - non-i.i.d.	
	Acc. (%)	Loss	Acc. (%)	Loss	Acc. (%)	Loss
4.0	58.05	1.152	48.22	1.473	37.58	1.724
2.0	63.27	1.041	51.90	1.403	40.35	1.638
1.0	65.18	1.044	54.66	1.325	41.34	1.594
0.5	64.19	1.030	53.19	1.320	41.52	1.551
0.25	63.88	1.092	54.64	1.265	43.41	1.532
0.05	60.98	1.227	47.60	1.701	44.71	1.528

Table 2: Average inference accuracy and model training loss for CIFAR10-CNN with different configurations. The impact of *FLex&Chill* is prominent for federated learning scenarios with non-i.i.d. datasets, whereas its impact is less than elsewhere.

We do point out that holding i.i.d. datasets in federated learning will show overall higher performance compared to non-i.i.d. configurations (regardless from T), but is not a practical case to assume when deploying federated learning systems. Rather, as we discussed, the impact of exploiting low training temperatures is beneficial when dealing with non-i.i.d. datasets.

4.6 Model stability of low-temperature training during federated learning aggregation

As discussed in Section 3, low temperatures expedite local training even with a small amount of training data. Nevertheless, the effect of low-temperature training on the model generalization and aggregation stability of federated learning has not yet been thoroughly studied. To inspect the stability of federated learning aggregation for models trained with low temperatures, we measured the performance change of each client-side model before and after the server-side aggregation round.

Thus, the pre-model performance will be high. However, since each model is trained aggressively over heterogeneous data, the aggregation process could puddle up this knowledge and the aggregated model may lose information. Ideally, with their local information properly aggregated, the performance drop will be minimal. Non-participating clients on the other hand, would hope to have an improved updated model of the federated learning process.

As Figure 7 shows the models trained with low temperatures retain the knowledge better than the medium and hot models for participating clients (solid plots groups at the bottom). In the early

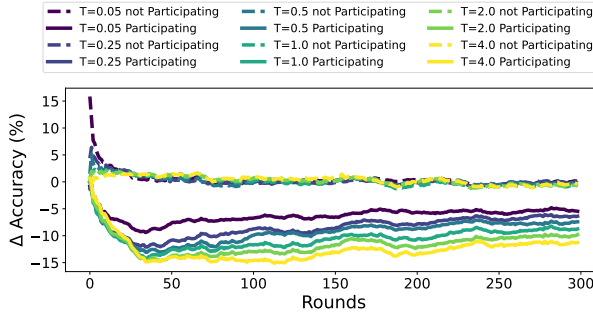


Figure 7: Accuracy drop observed before and after server-side model aggregation. The aggregation process of client models trained with lower temperatures better retains the individual knowledge.

Figure 7 plots the changes in accuracy observed for both participating and non-participating clients at each federated learning round. Specifically, once the model is aggregated, each client computes its accuracy with both the pre-update and the post-update model and computes their difference. Note that pre-update models for clients participating in the round would have updated their local models (very recently) with their own data.

rounds, the models with high temperatures show less performance drop, but the fast learning speed of the low-temperature model amortizes the performance drop, which results in faster learning of the aggregated model. Furthermore, we can also notice that the aggregation process does not interfere with the performance of non-participating clients (grouped on top), implying that federated learning with low-temperature training preserves the generalization power.

5 Discussion

- **Identifying the optimal temperature.** Our study exhibits the effectiveness of exploiting lower temperatures as a way to enhance federated learning performance. However, since the softmax layer training temperature can be considered a hyperparameter, optimal temperatures can vary depending on the applications and model architectures. Thus, like other hyperparameters used in model training (e.g., batch size, local epoch count), identifying an optimal temperature value is challenging to analytically solve, being beyond the scope of this paper.

Nevertheless, based on our experiences, we can offer heuristics for selecting temperatures regarding the model capacity and task complexity. Large capacity models with relatively easy tasks (e.g., low-resolution data, small number of labels to classify) often exhibit unstable convergence with low temperatures. We hypothesize that this phenomenon arises from lower temperatures compelling models to rapidly adapt to local data, which can potentially bias the model towards local data and disrupt the federated learning process. Thus, we carefully conclude our heuristics in two-fold. (i) Balancing the model capacity and task complexity is crucial to best leverage the temperature scaling during training; (ii) Large capacity models tend to work well with relatively high temperatures since they tend to suffer from instability with a too-low temperature.

- **Dynamic per-sample temperature scaling.** While our paper focuses on understanding the advantages of maintaining a *constant low temperature* for the training process, this may not be the ideal approach when targeting maximum performance. In reality, varying temperatures can be applied in the training process with respect to their significance Shin et al. [2022], Zeng et al. [2021]. That would mean that the training process can exploit lower temperatures for the samples that are “harder” to learn, while higher temperatures are used for those easier to understand. Alternatively, a more coarse-grain approach of dynamically adjusting the temperature on a per-federated learning round-basis can be another meaningful approach to adapt towards changing local data characteristics.

- **Supporting heterogeneous federated learning.** While many federated learning frameworks assume homogeneous devices, recent work points out that this is not always the case Park and Ko [2023]. In a federated learning network consisting of devices with heterogeneous computing/network capabilities, the issue of “stragglers”, which take longer to complete local training, becomes important to address. Leveraging insights gleaned from our empirical observations, applying lower temperatures for potential stragglers can be an interesting way of uniforming the local training duration. This would require a prior analysis on the conditions expected at each device and a global consensus on the temperature configuration. We find this as an interesting topic that requires further investigation.

6 Conclusion

This research introduces a novel training approach for federated learning systems, *FLex&Chill*, aimed at enhancing convergence and improving model performance by exploiting a temperature scaling

method termed *logit chilling* in federated learning local model training operations. Specifically, our work revolves around the implications of employing fractional temperature values ($T \in (0, 1)$) during the model training process. Our findings, derived from an extensive set of evaluations using three datasets and three widely applied neural networks for federated learning, demonstrate that exploiting the *FLex&Chill* approach in the client-side model training process holds the potential to expedite model convergence by inducing more pronounced changes despite a limited number of local samples. Consequently, we show that by doing so, we can also achieve an overall higher inference accuracy. While the impact of lower temperature varies with respect to the neural network architecture and dataset, our evaluations reveal up to $6.00\times$ improvement in federated learning model convergence speed and 3.37% improvement in inference accuracy. We see this work as a first step into devising a more fine-tuned (and optimal) training mechanism for federated learning systems.

References

- Brendan McMahan, Eider Moore, Daniel Ramage, Seth Hampson, and Blaise Aguera y Arcas. Communication-efficient learning of deep networks from decentralized data. In *Artificial intelligence and statistics*, pages 1273–1282. PMLR, 2017.
- JaeYeon Park, Kichang Lee, Sungmin Lee, Mi Zhang, and JeongGil Ko. Atfl: A personalized federated learning framework for time-series mobile and embedded sensor data processing. *Proceedings of the ACM on Interactive, Mobile, Wearable and Ubiquitous Technologies*, 7(3):1–31, 2023a.
- Yue Zhao, Meng Li, Liangzhen Lai, Naveen Suda, Damon Civin, and Vikas Chandra. Federated learning with non-iid data. *arXiv preprint arXiv:1806.00582*, 2018.
- Tian Li, Anit Kumar Sahu, Manzil Zaheer, Maziar Sanjabi, Ameet Talwalkar, and Virginia Smith. Federated optimization in heterogeneous networks. *Proceedings of Machine learning and systems*, 2:429–450, 2020.
- Sai Praneeth Karimireddy, Satyen Kale, Mehryar Mohri, Sashank Reddi, Sebastian Stich, and Ananda Theertha Suresh. Scaffold: Stochastic controlled averaging for federated learning. In *International conference on machine learning*, pages 5132–5143. PMLR, 2020.
- Geoffrey Hinton, Oriol Vinyals, and Jeff Dean. Distilling the knowledge in a neural network. *arXiv preprint arXiv:1503.02531*, 2015.
- Hugo Touvron, Matthieu Cord, Matthijs Douze, Francisco Massa, Alexandre Sablayrolles, and Hervé Jégou. Training data-efficient image transformers & distillation through attention. In *International conference on machine learning*, pages 10347–10357. PMLR, 2021.
- Chuan Guo, Geoff Pleiss, Yu Sun, and Kilian Q Weinberger. On calibration of modern neural networks. In *International conference on machine learning*, pages 1321–1330. PMLR, 2017.
- JaeYeon Park, Kichang Lee, Noseong Park, Seng Chan You, and JeongGil Ko. Self-attention lstm-fcn model for arrhythmia classification and uncertainty assessment. *Artificial Intelligence in Medicine*, 142:102570, 2023b.
- Tim Pearce, Alexandra Brintrup, and Jun Zhu. Understanding softmax confidence and uncertainty. *arXiv preprint arXiv:2106.04972*, 2021.
- Eric Jang, Shixiang Gu, and Ben Poole. Categorical reparameterization with gumbel-softmax. *arXiv preprint arXiv:1611.01144*, 2016.
- Andy Shih, Dorsa Sadigh, and Stefano Ermon. Long horizon temperature scaling. *arXiv preprint arXiv:2302.03686*, 2023.
- Pei-Hsin Wang, Sheng-Iou Hsieh, Shih-Chieh Chang, Yu-Ting Chen, Jia-Yu Pan, Wei Wei, and Da-Chang Juan. Contextual temperature for language modeling. *arXiv preprint arXiv:2012.13575*, 2020.
- Fuxun Yu, Weishan Zhang, Zhuwei Qin, Zirui Xu, Di Wang, Chenchen Liu, Zhi Tian, and Xiang Chen. Fed2: Feature-aligned federated learning. In *Proceedings of the 27th ACM SIGKDD conference on knowledge discovery & data mining*, pages 2066–2074, 2021.

- Lumin Liu, Jun Zhang, SH Song, and Khaled B Letaief. Client-edge-cloud hierarchical federated learning. In *ICC 2020-2020 IEEE International Conference on Communications (ICC)*, pages 1–6. IEEE, 2020.
- Alex Krizhevsky, Geoffrey Hinton, et al. Learning multiple layers of features from tiny images. 2009.
- Utku Evci, Yani Ioannou, Cem Keskin, and Yann Dauphin. Gradient flow in sparse neural networks and how lottery tickets win. In *Proceedings of the AAAI conference on artificial intelligence*, volume 36, pages 6577–6586, 2022.
- Juyeop Kim, Junha Park, Songkuk Kim, and Jong-Seok Lee. Curved representation space of vision transformers. *arXiv preprint arXiv:2210.05742*, 2022.
- Ian J Goodfellow, Jonathon Shlens, and Christian Szegedy. Explaining and harnessing adversarial examples. *arXiv preprint arXiv:1412.6572*, 2014.
- Sebastian Caldas, Sai Meher Karthik Duddu, Peter Wu, Tian Li, Jakub Konečný, H Brendan McMahan, Virginia Smith, and Ameet Talwalkar. Leaf: A benchmark for federated settings. *arXiv preprint arXiv:1812.01097*, 2018a.
- Gregory Cohen, Saeed Afshar, Jonathan Tapson, and Andre Van Schaik. Emnist: Extending mnist to handwritten letters. In *2017 international joint conference on neural networks (IJCNN)*, pages 2921–2926. IEEE, 2017.
- Sebastian Caldas, Sai Meher Karthik Duddu, Peter Wu, Tian Li, Jakub Konečný, H Brendan McMahan, Virginia Smith, and Ameet Talwalkar. GitHub - TalwalkarLab/leaf: Leaf: A Benchmark for Federated Settings — github.com. <https://github.com/TalwalkarLab/leaf>, 2018b.
- Kaiming He, Xiangyu Zhang, Shaoqing Ren, and Jian Sun. Deep residual learning for image recognition. In *Proceedings of the IEEE conference on computer vision and pattern recognition*, pages 770–778, 2016.
- Sebastian Ruder. An overview of gradient descent optimization algorithms. *arXiv preprint arXiv:1609.04747*, 2016.
- Simon Kornblith, Mohammad Norouzi, Honglak Lee, and Geoffrey Hinton. Similarity of neural network representations revisited. In *International conference on machine learning*, pages 3519–3529. PMLR, 2019.
- Liam Collins, Hamed Hassani, Aryan Mokhtari, and Sanjay Shakkottai. Fedavg with fine tuning: Local updates lead to representation learning. *Advances in Neural Information Processing Systems*, 35:10572–10586, 2022.
- Mi Luo, Fei Chen, Dapeng Hu, Yifan Zhang, Jian Liang, and Jiashi Feng. No fear of heterogeneity: Classifier calibration for federated learning with non-iid data. *Advances in Neural Information Processing Systems*, 34:5972–5984, 2021.
- Tzu-Ming Harry Hsu, Hang Qi, and Matthew Brown. Measuring the effects of non-identical data distribution for federated visual classification. *arXiv preprint arXiv:1909.06335*, 2019.
- Jaemin Shin, Yuanchun Li, Yunxin Liu, and Sung-Ju Lee. Fedbalancer: data and pace control for efficient federated learning on heterogeneous clients. In *Proceedings of the 20th Annual International Conference on Mobile Systems, Applications and Services*, pages 436–449, 2022.
- Xiao Zeng, Ming Yan, and Mi Zhang. Mercury: Efficient on-device distributed dnn training via stochastic importance sampling. In *Proceedings of the 19th ACM Conference on Embedded Networked Sensor Systems*, pages 29–41, 2021.
- JaeYeon Park and JeongGil Ko. Fedhm: Practical federated learning for heterogeneous model deployments. *ICT Express*, 2023. ISSN 2405-9595. doi: <https://doi.org/10.1016/j.ict.2023.07.013>. URL <https://www.sciencedirect.com/science/article/pii/S2405959523000929>.

Adam Paszke, Sam Gross, Francisco Massa, Adam Lerer, James Bradbury, Gregory Chanan, Trevor Killeen, Zeming Lin, Natalia Gimelshein, Luca Antiga, Alban Desmaison, Andreas Kopf, Edward Yang, Zachary DeVito, Martin Raison, Alykhan Tejani, Sasank Chilamkurthy, Benoit Steiner, Lu Fang, Junjie Bai, and Soumith Chintala. Pytorch: An imperative style, high-performance deep learning library. In *Advances in Neural Information Processing Systems 32*, pages 8024–8035. Curran Associates, Inc., 2019. URL <http://papers.neurips.cc/paper/9015-pytorch-an-imperative-style-high-performance-deep-learning>

A Gradient of softmax with varying temperature

Proof. Let cross-entropy loss for softmax as $\mathcal{L} = -\sum_{j=1}^C y_j \log(p_j)$, where C is the number of classes and y_j and p_j corresponds to the hard label (i.e., onehot-encoded label) and probability for given class. Here, the probability p_j is computed by exploiting the softmax with varying temperatures which can be formalized as follows.

$$p_j = \frac{e^{z_j/T}}{\sum_{i=1}^C e^{z_i/T}}$$

Here, T is the temperature, and z_j is the logit used as the input of the softmax function.

$$\begin{aligned}
 \frac{\partial \mathcal{L}}{\partial z_i} &= -\sum_{j=1}^C \frac{\partial y_j \log(p_j)}{\partial z_i} \\
 &= \sum_{j=1}^C y_j \frac{\partial \log(p_j)}{\partial z_i} \\
 &= -\sum_{j=1}^C y_j \frac{\partial \log(p_j)}{\partial z_i} \\
 &= -\sum_{j=1}^C y_j \frac{1}{p_j} \frac{\partial p_j}{\partial z_i} \\
 &= -\frac{y_i}{p_i} \frac{\partial p_i}{\partial z_i} - \sum_{j \neq i}^C \frac{y_j}{p_j} \frac{\partial p_j}{\partial z_i} \\
 &= -\frac{y_i}{p_i} \frac{1}{T} p_i (1 - p_i) - \sum_{j \neq i}^C \frac{y_j}{p_j} (-p_j p_i) \\
 &= -\frac{y_i}{T} + \frac{1}{T} y_i p_i + \frac{1}{T} \sum_{j \neq i}^C y_j p_i \\
 &= -\frac{y_i}{T} + \frac{1}{T} \sum_{j=1}^C y_j p_i \\
 &= -\frac{y_i}{T} + \frac{1}{T} p_i \sum_{j=1}^C y_j \\
 &= \frac{1}{T} (p_i - y_i) \\
 \therefore \frac{\partial \mathcal{L}}{\partial z_i} &= \frac{1}{T} (p_i - y_i) \\
 &= \frac{1}{T} \left(\frac{e^{z_i/T}}{\sum_j e^{z_j/T}} - y_i \right)
 \end{aligned}$$

□

B Experimental Details

B.1 Model Architecture

Layer	Details	Repetition
FC 1	Linear(784, 512) ReLU()	×1
FC 2	Linear(512, 256) ReLU()	×1
FC 3	Linear(256, 128) ReLU()	×1
FC 4	Linear(256, 62)	×1

Table 3: Model architectures details of DNN used to train the FEMNIST dataset

Layer	Details	Repetition
Conv 1	Conv2d(3, 10, k=(5, 5), s=(1, 1))	×1
	ReLU()	
	MaxPool2d(k=(2, 2))	
Conv 2	Conv2d(10, 20, k=(5, 5), s=(1, 1))	×1
	ReLU()	
	MaxPool2d(k=(2, 2))	
FC 1	Linear(500, 256)	×1
	ReLU()	
FC 2	Linear(256, 10)	×1

Table 4: Model architectures details of 2-layered CNN used to train the CIFAR10 dataset

For the ResNet18 model used to train the CIFAR100 dataset, we exploited PyTorch implementation Paszke et al. [2019] by only replacing the final classification head from Linear(512, 1000) to Linear(512, 100).

B.2 Hyperparameters

Hyperparameters	FEMNIST-DNN	CIFAR10-CNN	CIFAR100-ResNet18	CKA Evaluation
total clients	36		50	10
communication rounds		300		100
optimizer		SGD		
learning rate		0.001		0.005
local epoch		10		10
participants per round		10		10
batch size		16		32
shard size l α	N/A		200	$\alpha=0.5$
loss function		Cross Entropy		

Table 5: Hyperparameters used for Section 4. α denotes the importance of the Dirichlet distribution.

B.3 Data distribution

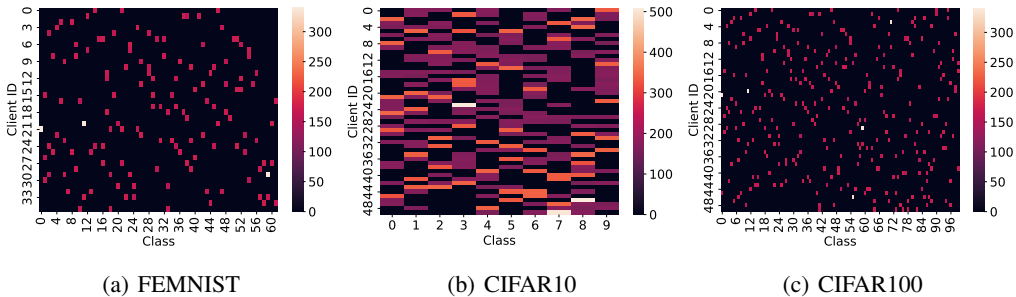


Figure 8: Visualization of the distribution of training data used in FEMNIST, CIFAR10-CNN and CIFAR100-ResNet experiments. Best viewed in color.

B.4 Hardware

For the experiments, we exploited server with four GeForce RTX 2080 Ti GPUs, Intel(R) Xeon(R) Silver 4210 CPU @ 2.20GHz, and 64GB RAM.

C Orthogonality of *FLex&Chill*

C.1 *FLex&Chill* As An Algorithm

We formulate the operations of *FLex&Chill* using Algorithm 1. Here, typical federated learning operations take place at both the server and clients except for the fact that the server determines a target T at each round and local model training operations are performed with T . Since *FLex&Chill* only manipulates the local training process which inherently provides orthogonality to our proposed method, it is extremely easy to integrate with existing federated learning frameworks.

Algorithm 1 *FLex&Chill*

Data (D_1, D_2, \dots, D_N) where D_i is the user i 's local data.

Model ($w_t^1, w_t^2, \dots, w_t^N$) where w_t^i is the user i 's model in t -th federated round.

Parameter: Temperature $T \in (0, 1)$

```

1: Server executes:
2: Initialize  $w_0$ 
3: for each round  $t = 1, 2, \dots, R$  do
4:    $S_t \leftarrow$  (random set of  $m$  clients)
5:   for  $k \in S_t$  do
6:      $w_t^k \leftarrow$  ClientUpdate( $w_t, T$ )
7:   end for
8:   for  $k \in S_t$  do
9:      $w_{t+1} \leftarrow$  Aggregation( $w_t^k$ )
10:  end for
11: end for
12: ClientUpdate( $w_t, T$ ):
13:  $w_t^k \leftarrow w_t$ 
14: for data, label  $\in D_k$  do
15:    $\mathbf{z} = w_t^k(\text{data})/T$ 
16:    $l(\mathbf{z}) = \text{loss}(\mathbf{z}; \text{label})$ 
17:    $w_t^k \leftarrow$  LocalUpdate( $w_t^k, l(\mathbf{z})$ )
18: end for
19: Return  $w_t^k$  to server

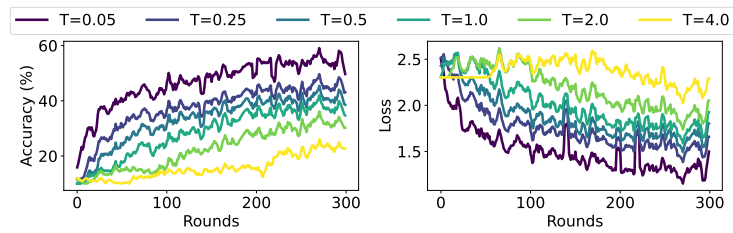
```

C.2 *FLex&Chill* with Advanced FL Schemes

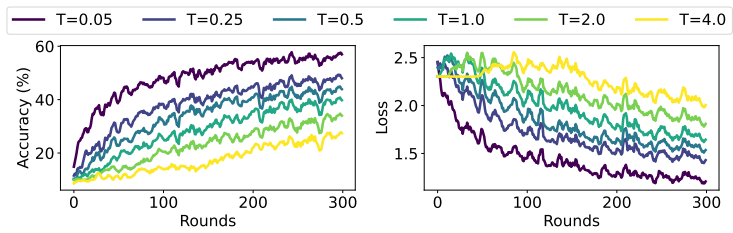
As mentioned in Section 3.2, *FLex&Chill* is an orthogonal approach to enhance the federated learning process. To demonstrate this, we trained the 2-layer CNN with FedProx Li et al. [2020] and SCAFFOLD Karimireddy et al. [2020] representing more recently proposed FL schemes compared to FedAvg used in this work.

Hyperparameters	FedProx	SCAFFOLD
total clients		50
communication rounds		300
optimizer		SGD
learning rate		0.001
local epoch		5
participants per round		5
batch size		32
α		0.5
loss function		Cross Entropy
μ	0.01	N/A

Table 6: Default hyperparameters used in this section. α denotes the importance of the Dirichlet distribution.



(a) FedProx



(b) SCAFFOLD

Figure 9: Test accuracy and test loss on the CIFAR10 dataset with varying training temperatures with advanced federated learning schemes. Overall, models trained with lower temperatures showed superior performance.

D Experiment on hyperparameters

In this section, we explore the effect of other federated learning hyperparameters (i.e., batch size, number of local epochs, number of participants, and degree of data disparity). Through this set of experiments, we observed that applying low temperatures during local training improves test accuracy and convergence speed, being independent from hyperparameters. We note that the experiments were done by applying the default setting except for the control factors.

D.1 Batch size

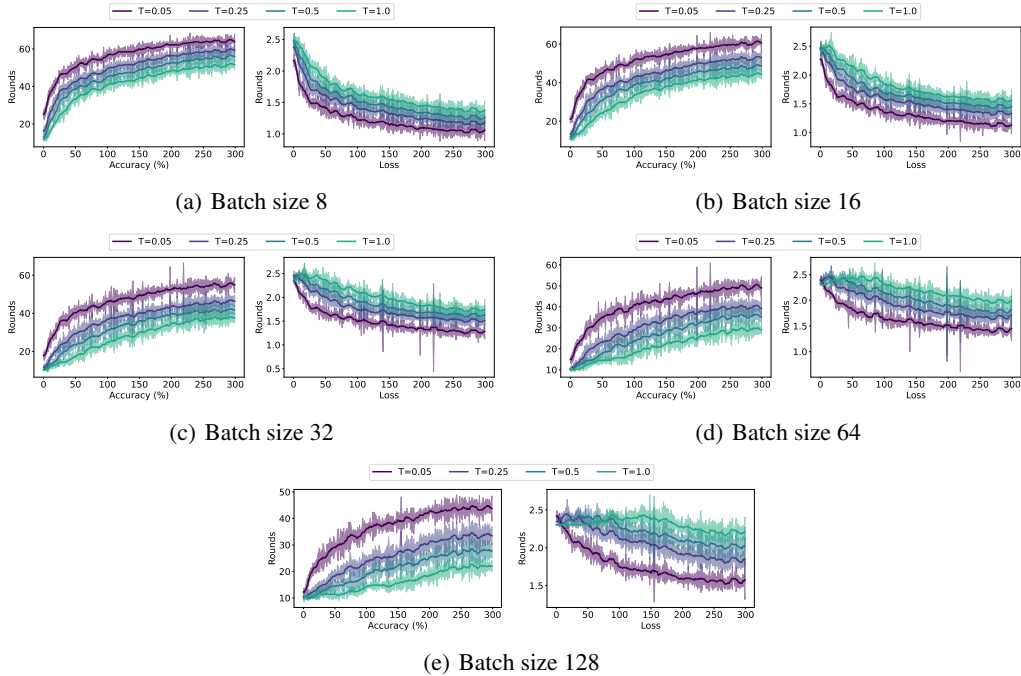


Figure 10: Test accuracy and test loss over federated learning round with varying the batch size and the training temperature on the CIFAR10 dataset. Relatively small batch size shows better training quality with stability.

D.2 Number of participants

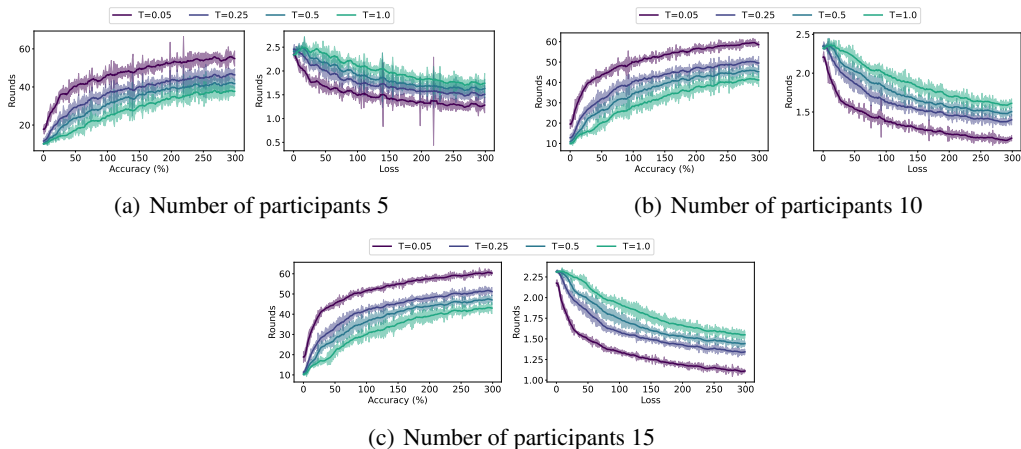


Figure 11: Test accuracy and test loss over federated learning round with varying the number of participants and the training temperature on the CIFAR10 dataset. When relatively many clients participate in the training, it shows better training quality with stability

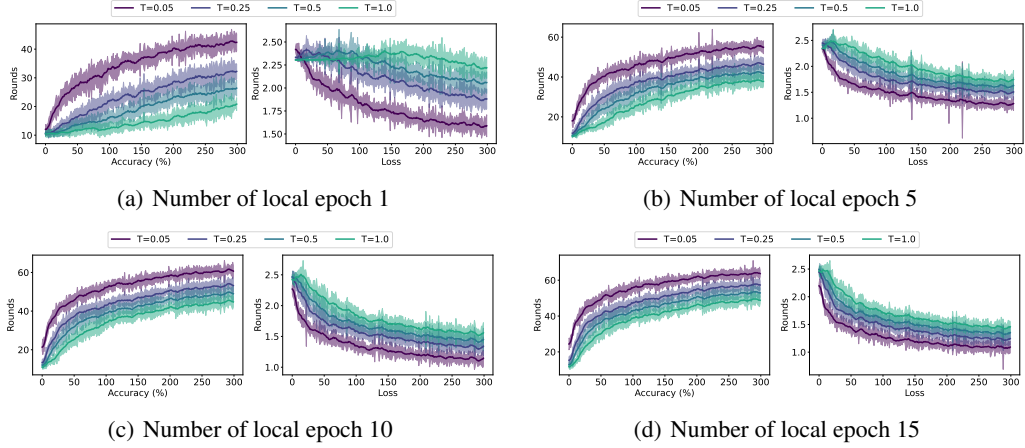


Figure 12: Test accuracy and test loss over federated learning round with varying the number of local epochs and the training temperature on the CIFAR10 dataset. Relatively many updates in the local training phase show better training quality with stability

D.3 Number local epochs

D.4 Degree of data disparity

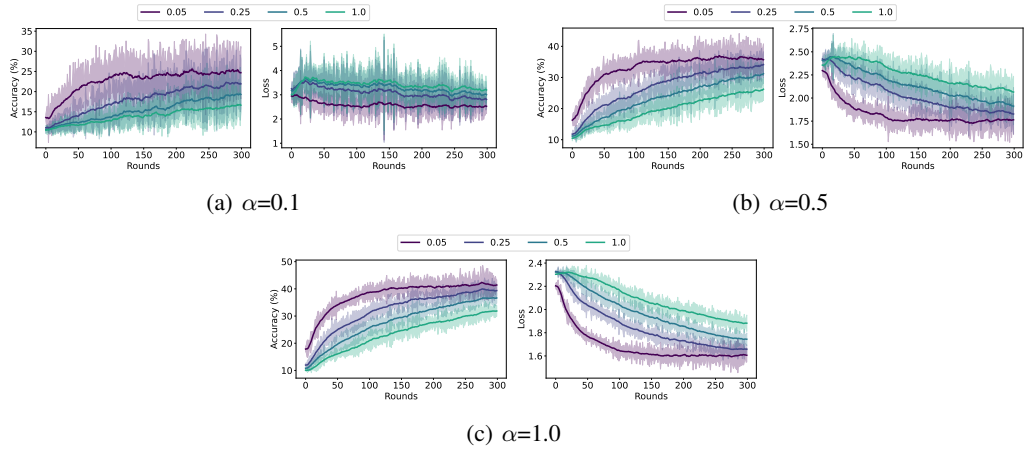


Figure 13: Test accuracy and test loss over federated learning round with varying the degree of data disparity and the training temperature on the CIFAR10 dataset. Relatively moderate data disparity shows better training quality with stability

Hyperparameters	Appendix D
total clients	50
communication rounds	100
optimizer	SGD
learning rate	0.001
local epoch	5
participants per round	5
batch size	32
α	0.5
loss function	Cross Entropy

Table 7: Default hyperparameters used in this section. α denotes the importance of the Dirichlet distribution.

E Details of Centered Kernel Alignment (CKA)

E.1 Background

Centered kernel alignment (CKA) is a method to compute the similarity between two different neural networks by measuring the similarity of the network representation for the given input data. Let X and Y be the features generated from two different neural networks, we can calculate the CKA by Eq 3. As we are assuming a federated learning scenario, the clients share the same neural network architecture. Thus, the dimensions of the two features from each corresponding layer are identical, allowing for a direct comparison to be possible. We note that in our experiments, we exploited the linear CKA to measure the similarity of the feature spaces between two neural networks.

$$CKA(X, Y) = \frac{\|Y^T X\|_F^2}{\|X^T X\|_F \|Y^T Y\|_F} \quad (3)$$

E.2 Limitation of Centered Kernel Alignment evaluation in federated learning

Here, we discuss our rationale for measuring CKA between a client model participating in the federated learning round and a reference model trained using i.i.d. configurations. As mentioned in Section 4.4, the feature space similarity itself only reports the similarity of neural networks and *does not assure high quality (i.e., accuracy) of the trained models*. Figure 14 illustrates the possible cases that can be observed in a federated learning scenario. We use these four cases to understand how locally trained models converge to the reference model. Here, the orange line indicates the update directions of local models from the federated learning training phase (i.e., diverging from the initially shared aggregated model presented as the black dot) and the red dotted line represents the average of these locally updated models that occur at the server. The star represents the ideal model in the representation space with high accuracy.

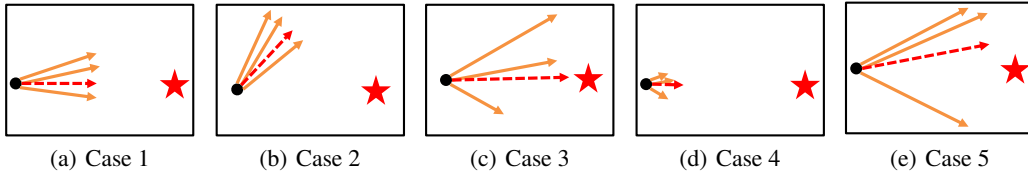


Figure 14: Illustration of possible cases in a federated learning scenario. The solid orange line and dotted red line correspond to the local update direction and aggregated model update direction respectively. The black circle and the red star depict the initial point and optimal point respectively.

- High similarity between local models does not guarantee a better model (Case 1, 2):** The first case arises when local models, each trained on their respective local data, produce highly similar updates due to a well-aligned data configuration. Such alignment implies that the training data across different clients are relatively similar in distribution and characteristics, allowing the aggregated global model to closely approach the ideal model achievable through centralized training. However, in non-i.i.d. environments, achieving this scenario is infrequent. In non-i.i.d. settings, the data distribution varies significantly across different local nodes. This variation can lead to local models learning disparate aspects of the data, resulting in updates that are less similar. Consequently, the aggregated global model may not perform as well as in an i.i.d. scenario, as it has to reconcile these diverse and potentially conflicting updates. On the other hand, Case 2 represents a critical scenario in federated learning where there is a high similarity among local model updates, but these updates are aligned in a suboptimal or incorrect direction. This situation can be considered one of the worst cases in federated learning. In addition, using these two cases, we demonstrate that the high similarity between local models does not ensure a superior update or quality of training.

- A superior model can be obtained without similar local models (Case 3):** Case 3 illustrates a case where a superior model can be achieved even when local models exhibit relatively low similarity. In this scenario, each local model learns effective but diverse features from heterogeneous data configurations, and these diverse updates are properly aggregated at the central server. Unlike scenarios where local models produce highly similar updates, in this case, the updates from different

local models show significant variation. This diversity reflects the different aspects of the data each local model has learned. This situation arises under conditions of data heterogeneity, where the data distributions across different clients are diverse. Each local model captures unique features relevant to its specific data subset. Despite the low similarity among local model updates, the central server effectively aggregates these diverse updates. The aggregation process leverages the complementary information from each local model, resulting in a robust and well-generalized global model. This case supports the hypothesis that a proper global model can be obtained even when local models do not exhibit high similarity and is a globally ideal case for federated learning scenarios.

• **Relationship between model similarity and the magnitude of updates (Case 4, 5):** It is important to note that the magnitude of updates can influence the perceived similarity of the network. If the update magnitude is small, the similarity of the network may be measured as high, whereas if the update magnitude is large, the similarity may be measured as relatively low. This example underscores the need to rethink the conventional emphasis on high similarity as an indicator of performance. It suggests that focusing solely on similarity metrics, while providing insights on how local training operations induce model changes, might overlook other critical factors that contribute to the effectiveness of the aggregated model. Therefore, a more nuanced approach to evaluating model updates and their impact on the accuracy performance is required, considering both the magnitude of updates and their alignment with the overall learning objectives.

Based on the aforementioned discussions, we introduce measuring similarity with a reference model as an alternative evaluation method in this work. Although we cannot ensure that the reference model trained in an i.i.d. data configuration perfectly represents the optimal update objective, we consider this method as an effective and reasonable way to evaluate the federated learning process. This approach allows for a more nuanced assessment of the updates by comparing them to a standard benchmark, helping to identify whether the aggregated model is progressing toward a semi-optimal solution despite the inherent data heterogeneity.

E.3 Experimental results

Table 8 presents the exact numbers for the accuracy and CKA values discussed in Section 4.4 and Figure 5. Figure 15 illustrates the data distribution applied in the experiments.

Temperature (T)	Accuracy (%)	Layer 1 CKA	Layer 2 CKA	Layer 3 CKA	Layer 4 CKA
4.00	49.72	0.6539	0.5632	0.7149	0.7661
2.00	53.82	0.6792	0.6872	0.7417	0.7963
1.00	58.19	0.7419	0.6997	0.7644	0.8214
0.50	63.48	0.9322	0.7459	0.8181	0.8559
0.25	66.85	0.9569	0.8161	0.8418	0.8830
0.05	72.76	0.9390	0.9059	0.8898	0.9026
Reference Model ($T=1.00$, i.i.d.)	73.86	1.0000	1.0000	1.0000	1.0000

Table 8: Accuracy and CKA values of 2 layer CNN measured on the CIFAR10 dataset in Figure 5.

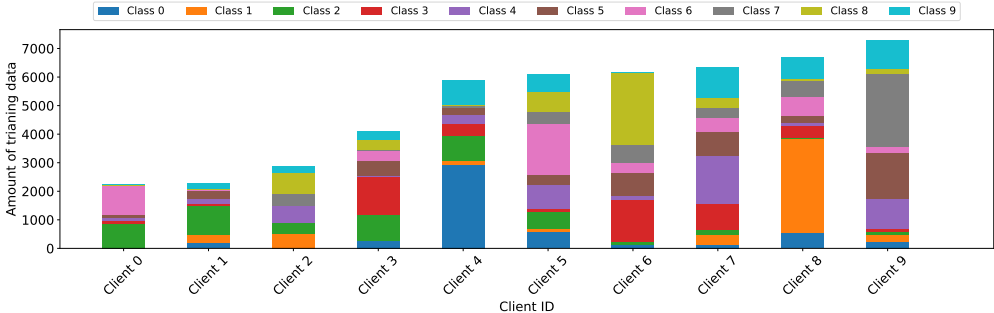


Figure 15: Visualization of the distribution of training data used in CKA evaluation. Best viewed in color.

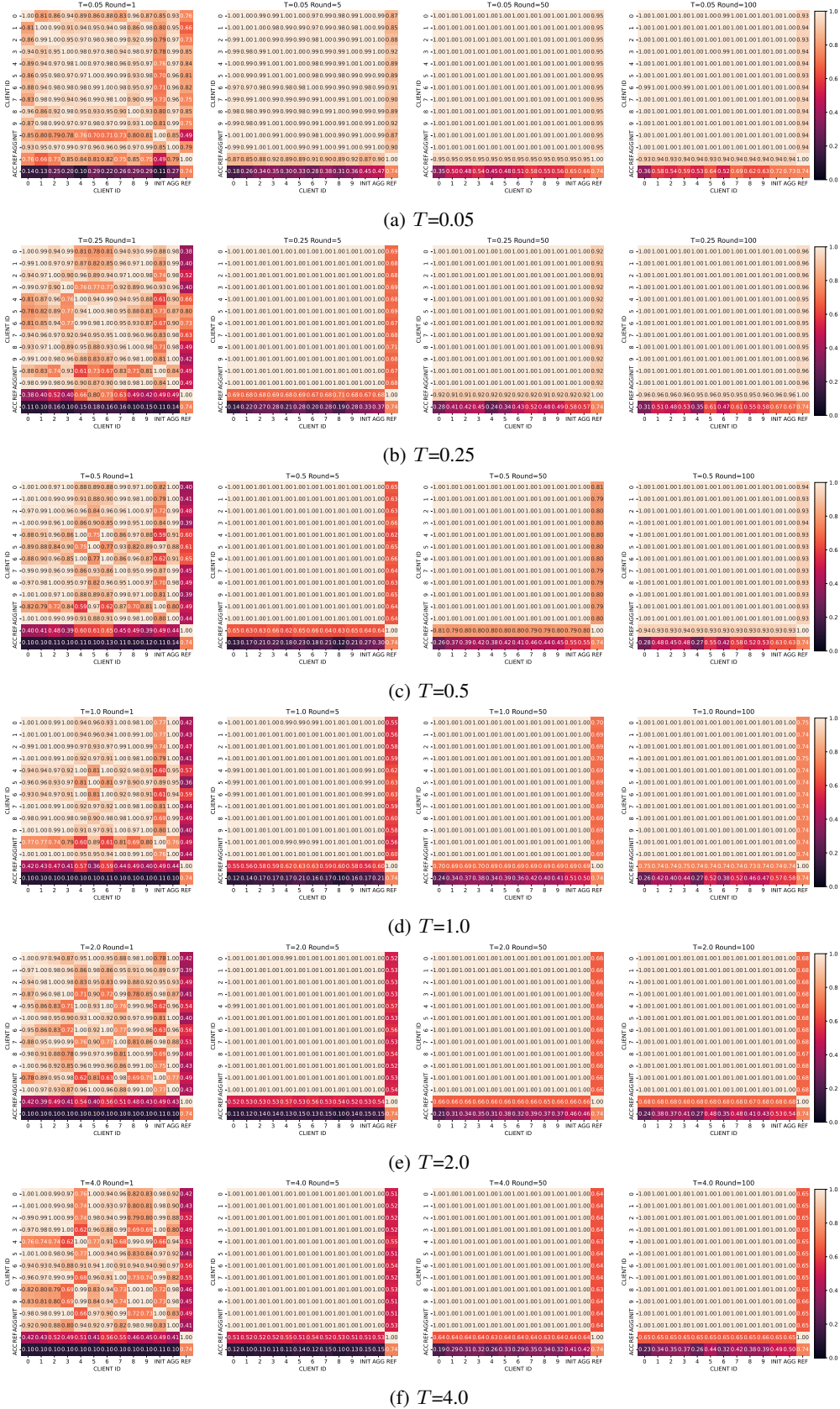
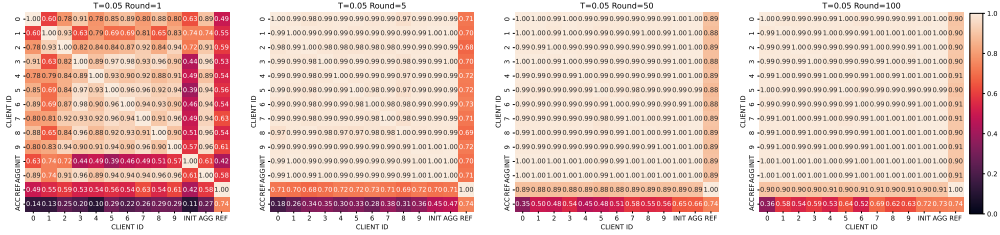
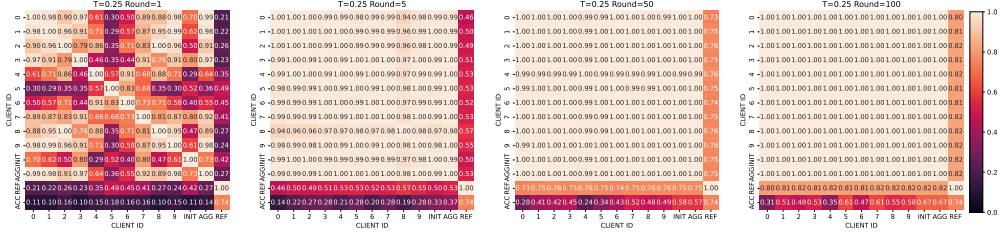


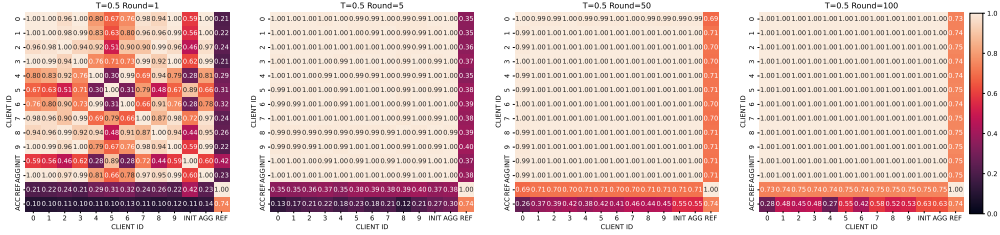
Figure 16: Client-wise feature space similarity matrix measured in the first convolution layers (Layer 1) by using CKA and inference accuracy at different temperatures (0.05, 0.25, 0.5, 1.0, 2.0, 4.0) and federated rounds (1, 5, 50, 100). (INIT: Initial dispatched model in the given round, AGG: Aggregated global model, REF: Reference model, ACC: Accuracy)



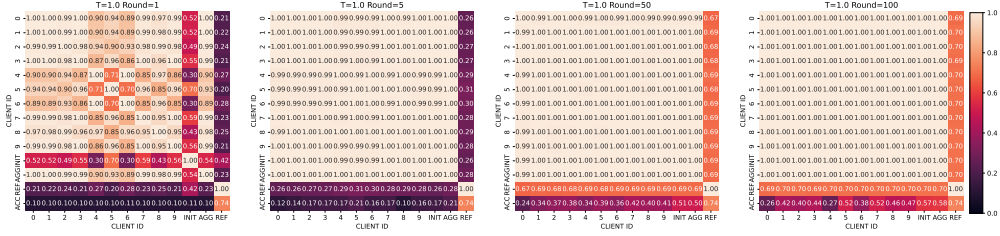
(a) $T=0.05$



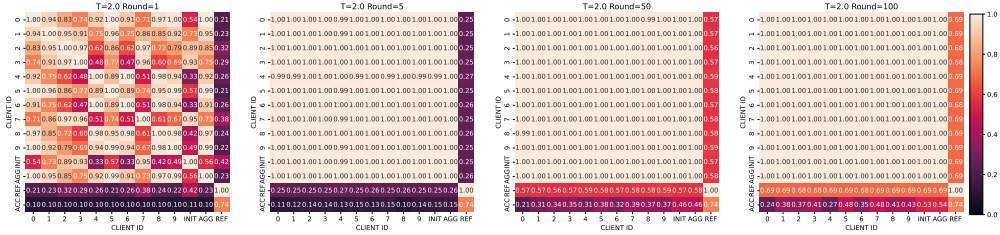
(b) $T=0.25$



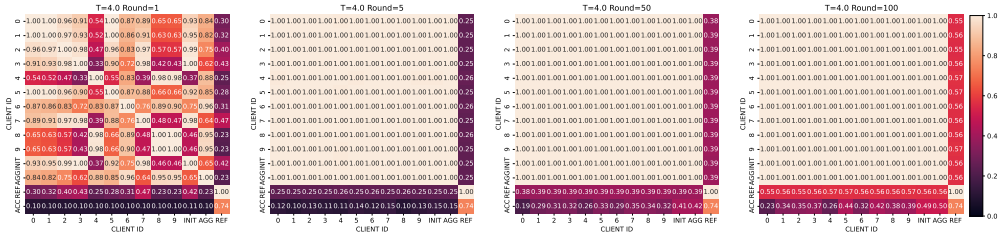
(c) $T=0.5$



(d) $T=1.0$



(e) $T=2.0$



(f) $T=4.0$

Figure 17: Client-wise feature space similarity matrix measured in the second convolution layers (Layer 2) by using CKA and inference accuracy in different temperatures (0.05, 0.25, 0.5, 1.0, 2.0, 4.0) and federated rounds (1, 5, 50, 100). (INIT: Initial dispatched model in the given round, AGG: Aggregated global model, REF: Reference model, ACC: Accuracy)

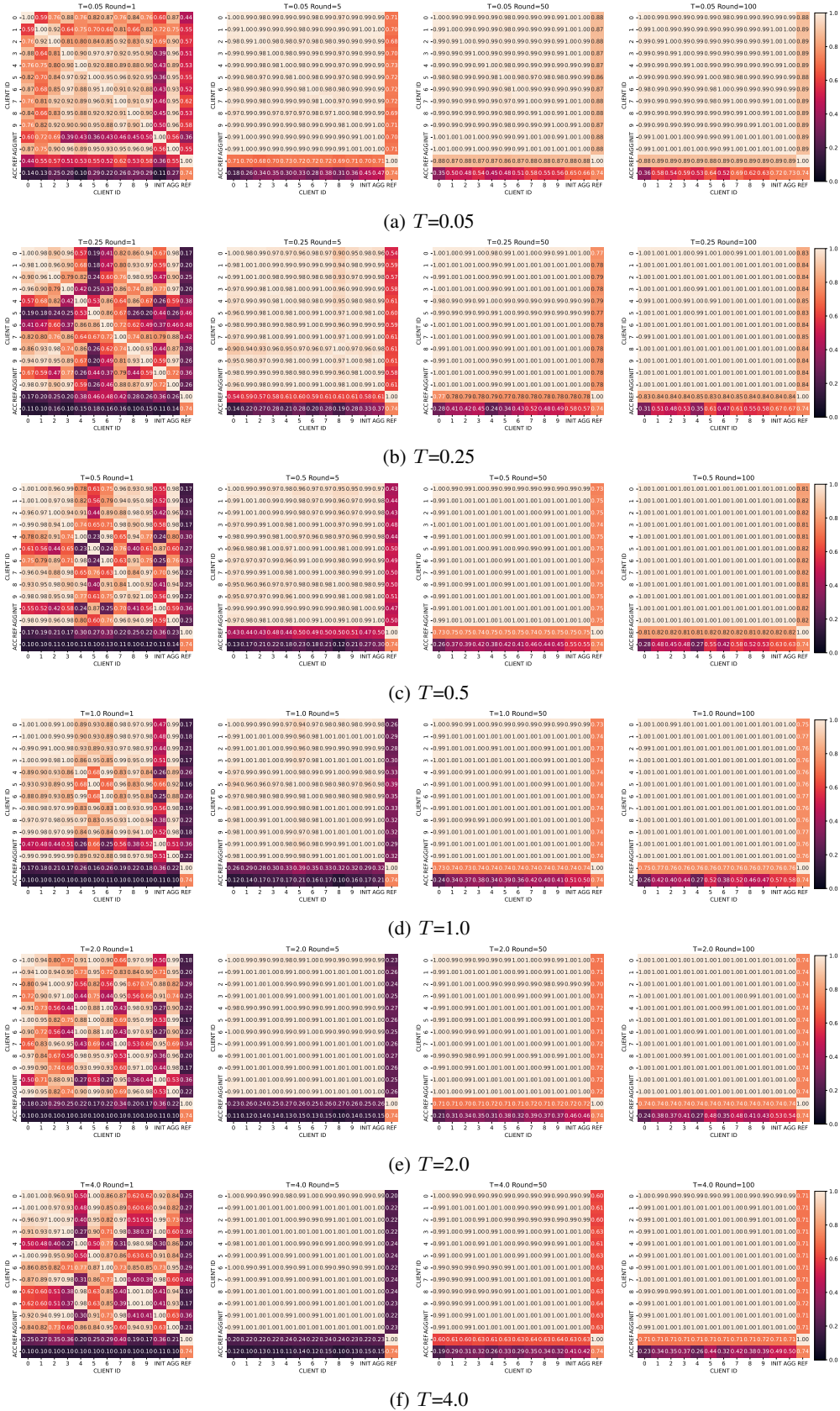
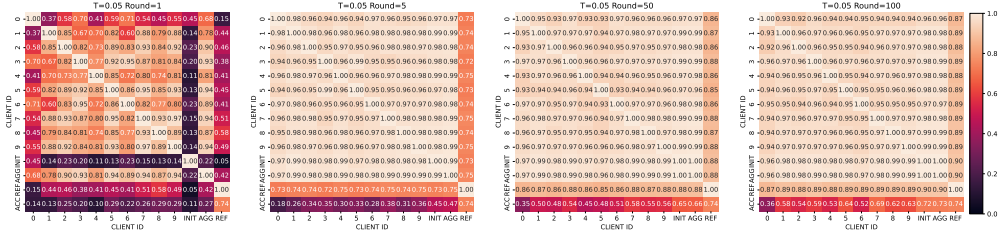
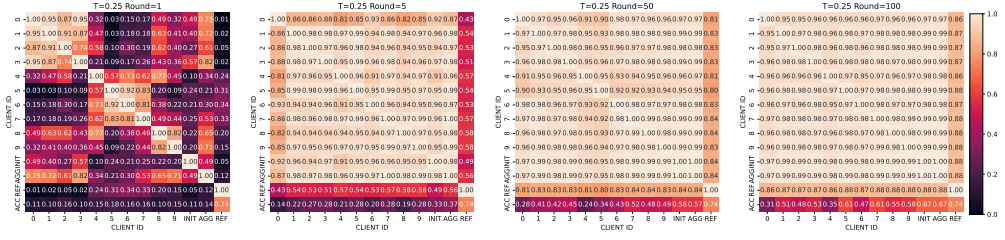


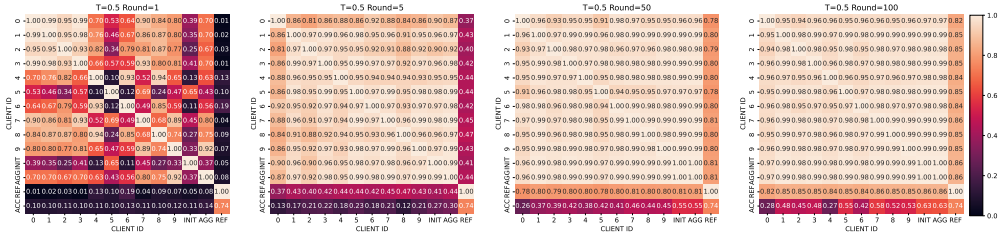
Figure 18: Client-wise feature space similarity matrix measured in penultimate layers (Layer 3) by using CKA and inference accuracy in different temperatures (0.05, 0.25, 0.5, 1.0, 2.0, 4.0) and federated rounds (1, 5, 50, 100). (INIT: Initial dispatched model in the given round, AGG: Aggregated global model, REF: Reference model, ACC: Accuracy)



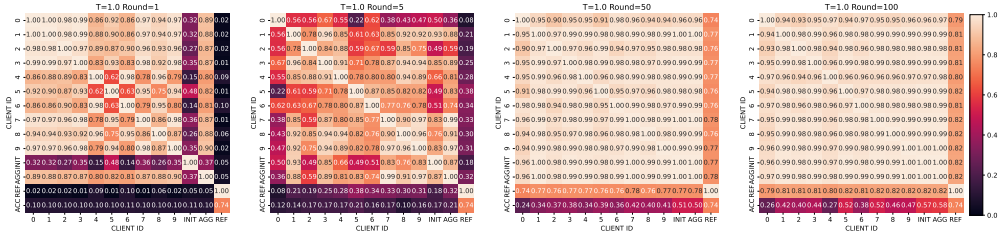
(a) $T=0.05$



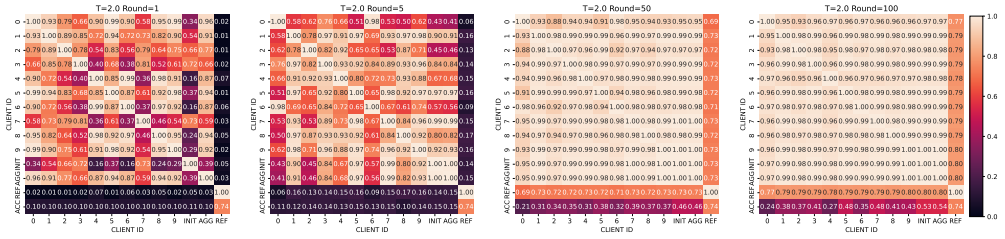
(b) $T=0.25$



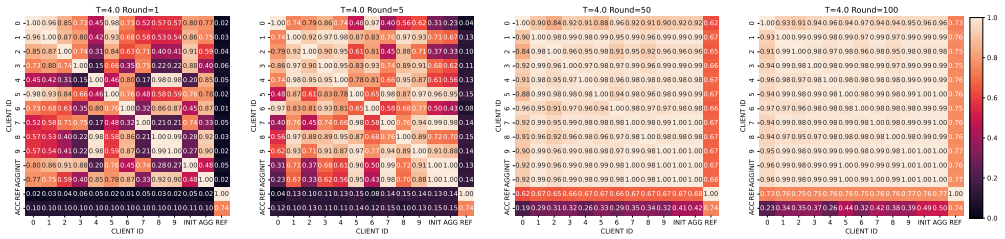
(c) $T=0.5$



(d) $T=1.0$



(e) $T=2.0$



(f) $T=4.0$

Figure 19: Client-wise feature space similarity matrix measured in classification layers (Layer 4) by using CKA and inference accuracy in different temperatures (0.05, 0.25, 0.5, 1.0, 2.0, 4.0) and federated rounds (1, 5, 50, 100). (INIT: Initial dispatched model in the given round, AGG: Aggregated global model, REF: Reference model, ACC: Accuracy)